inorganics

MDPI

Article

The Decomposition Products of Sulfur Hexafluoride (SF_6) with Metals Dissolved in Liquid Ammonia

Holger Lars Deubner and Florian Kraus *

Fachbereich Chemie, Philipps-Universität Marburg, 35043 Marburg, Germany;
lars.deubner@chemie.uni-marburg.de

* Correspondence: florian.kraus@chemie.uni-marburg.de; Tel.: +49-6421-28-26668

Received: 25 September 2017; Accepted: 11 October 2017; Published: 13 October 2017

Abstract: Sulfur hexafluoride is a highly chemically inert gas with several important industrial applications. It is stable against fused alkali, oxygen and ammonia, even at several hundred degrees Celsius. In this work, the reactions between metals (Li–Cs, Sr, Ba, Eu, Yb) dissolved in liquid ammonia and SF_6 are reported, leading to mono- or bivalent fluorides and sulfides. To this end, SF_6 was passed into a cooled solution of the respective metal in liquid ammonia. The identity of the products was confirmed by powder X-ray diffraction and IR spectroscopy. The reactions could lead to a cheap and effective disposal method of the present amounts of stored SF_6, for possible generation of H_2S and HF.

Keywords: sulfur hexafluoride; metal; ammonia

1. Introduction

Sulfur hexafluoride, SF_6, is a colorless, nonflammable and highly inert gas with an extremely high global warming potential (GWP) [1,2]. Because of its excellent electric characteristics and high chemical stability, it is used as a dielectric medium in high-voltage circuit breakers, transformers, capacitors and many more industrial applications [3]. Since the search for a replacement material that is less harmful to the environment or that is easier to dispose of has not yet been successful, the decomposition of sulfur hexafluoride remains a current field of research [4–6].

The activation of SF_6 was first shown in the literature in 1900 by Moissan and Lebeau [7]. They described the reaction between sulfur hexafluoride and hydrogen sulfide to sulfur and hydrogen fluoride. Furthermore, reactions with elemental sodium at 200 °C and several catalytic activations with nickel- or rhodium-complexes of SF_6 have been published [4,5,8].

The reaction between SF_6 and sodium, dissolved in liquid ammonia, was reported in 1964 by Demitras and MacDiarmid; however, they were not able to identify the products [9]. The reaction between SF_6 and caesium in liquid ammonia at −61 °C gave several good hints as to the formation of CsF and Cs_2S [10].

$$8\ Cs + SF_6 \rightarrow 6\ CsF + Cs_2S \quad (1)$$

During the reaction of ⅛ mol SF_6 per 1 mol of Cs, they observed that the blue colour of the solution of Cs in NH_3 disappeared. The weight of the products compared to the weight of the reactants showed a ratio close to 1.14. This would be the expected ratio for the postulated reaction according to Equation (1). Dissolving the white-appearing products in water and adding some HCl leads to the formation of H_2S, which also represents an indication for the postulated reaction.

In the present work, the reaction between metals that dissolve in liquid ammonia at −60 °C and internal pressure and SF_6 were investigated in detail.

2. Results and Discussion

The reactions between the alkali metals dissolved in liquid ammonia and SF_6 lead to the formation of the respective products (Equation (2)) that Demitras and MacDiarmid predicted for the reaction of Cs dissolved in NH_3 with SF_6.

$$8M^{I} + SF_6 \xrightarrow{-60\ ^{\circ}C,\ NH_3} M_2S + 6M^{I}F \quad (M = Li - Cs) \tag{2}$$

$$4M^{I} + SF_6 \xrightarrow{-60\ ^{\circ}C,\ NH_3} M^{II}S + 3MF_2 \quad (M = Sr, Ba, Eu) \tag{3}$$

The mono- or bivalent fluorides and sulfides could be obtained at −50 °C at reaction times ranging from nearly one to two and a half hours. The results are presented in the form of selected examples.

2.1. Alkali Metals (Li–Cs)

The conversion of SF_6 into alkali metal fluorides and the respective sulfides of the form $M^{I}F$ and M^{I}_2S took between 50 min for caesium (4.9 mmol) and 135 min for sodium (38 mmol). The reaction times and turnover rates for the reaction are shown in Table 1. During the reaction the blue to bronze colors of the solutions changed slowly to a light brownish white. The reaction rates did not correspond to the trend of rising reactivity of the alkali metals from Li to Cs, and the influence of the liquid ammonia solvent is also not clear. A precise control of the SF_6 gas flow by a flowmeter was not carried out.

Table 1. Reaction times and turnover rates for the reaction of alkali metals with SF_6.

	Li	Na	K	Rb	Cs
Reaction time [min]	130	135	90	75	50
Turnover rate [mmol/h]	16.6	17.2	6.80	6.66	5.85

After slowly removing the liquid ammonia under vacuum, a dark white to light brown powder remained in the Schlenk vessel. The powders were dried under vacuum at room temperature, and a powder X-ray diffraction pattern was recorded. The patterns showed rather broad reflexes over a large 2θ-range. A possible explanation for the broad reflexes are the small particle sizes. Recording an image with a scanning electron microscope (SEM) showed small particles with a diameter around or below 100 nm. One of these images of the product of the reaction between SF_6 and sodium is shown in Figure 1, and indicates a nano powder of NaF and Na_2S.

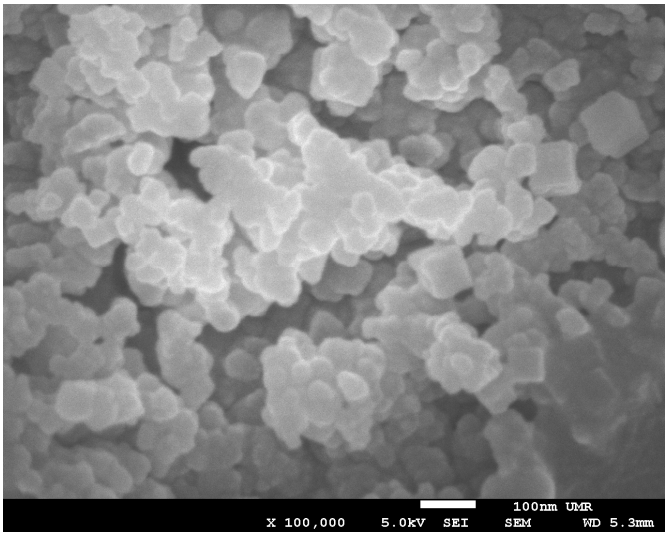

Figure 1. SEM image of the dried products of the reaction between SF_6 and Na.

For a better crystallization of the samples, a few hundred milligrams of the reaction mixture were sealed in a borosilicate tube and annealed under vacuum at 450 °C for five days. After crystallization, all X-ray powder diffraction patterns clearly showed the formation of the respective alkali metal fluoride $M^{I}F$. For sodium, potassium and rubidium, the characteristic reflections for the alkali metal sulfide M^{I}_2S were also observable. In some cases, the formation of the alkali metal amides as a byproduct was able to be shown by powder X-ray diffraction. For the reactions with lithium and caesium, the diffraction pattern only showed the formation of the respective fluoride and remnants of lithium metal. To prevent the formation of elemental sulfur, the powder was sealed into a borosilicate glass tube under vacuum (1.5×10^{-3} mbar) at a temperature gradient from 450 °C to room temperature. Because of its reactivity with glass, the products of the reaction between Li and SF_6 were sealed in a tantalum tube. A sublimation of elemental sulfur could not be observed. Another proof was the release of H_2S when immersed in diluted HCl, as shown by the blackening of moist $Pb(CH_3COO)_2$ paper.

Figure 2 shows the X-ray powder diffraction pattern of the reaction between Rb and SF_6. The *Rietfeld* refinement of the products, RbF and Rb_2S, shows a relation of RbF:Rb_2S of 88.0(1):12.0(1), which corresponds to the predicted value of 86:14. The lattice parameters are with a = 5.6586(1) Å, V = 181.187(4) Å^3 for RbF and a = 7.7533(2) Å, V = 466.080(8) Å^3 for Rb_2S in accordance with the results reported in the literature [11,12].

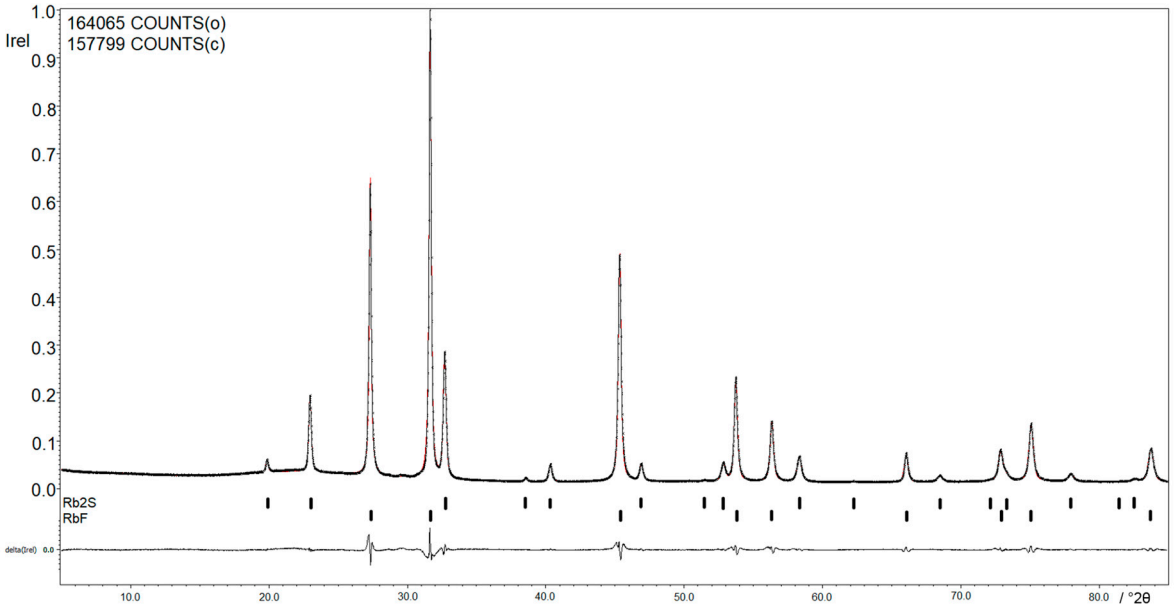

Figure 2. *Rietfeld* refinement of the X-ray powder diffraction pattern of RbF and Rb_2S. The calculated reflection positions are represented by strokes below the observed and calculated powder pattern. The difference curves are plotted underneath. Profile R factors: R_p = 3.95%, wR_p = 5.22%, GOF = 3.95.

As should be expected, the ATR IR spectrum of the mixture of RbF and Rb_2S (Figure S1) shows no bands in the range from 4000 to 400 cm^{-1}. An IR band of RbF should be observed at 376 cm^{-1}, so there is no IR activity expected in the measured region [13]. The measured intensities between 2200 and 1900 cm^{-1} are characteristic for the ATR diamond module.

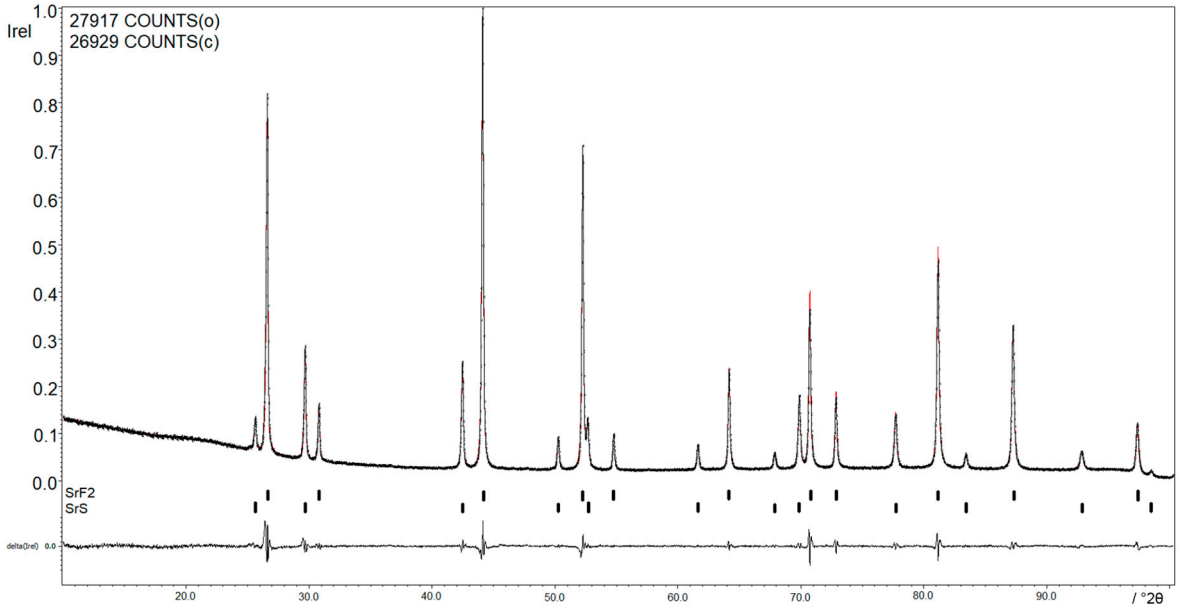

Figure 3. *Le Bail* fitting of the X-ray powder diffraction pattern of SrF_2 and SrS. The calculated reflection positions are represented by strokes below the observed and calculated powder pattern. The difference curves are plotted underneath. Profile *R* factors: R_p = 3.16%, wR_p = 4.40%, *GOF* = 1.72.

2.2. Alkaline Earth and Rare Earth Metals (Sr, Ba, Eu, Yb)

The conversion of SF_6 into the fluorides and sulfides of the form $M^{II}F_2$ and $M^{II}S$ with alkaline earth and rare earth metals took place for Ba, Sr and Eu, according to Equation (3). In the case of Yb, YbF_3 could also be obtained. The reaction times and turnover rates are shown in Table 2.

Table 2. Reaction times and turnover rates for the reaction of Sr, Ba, Eu and Yb with SF_6.

	Sr	Ba	Eu	Yb
Reaction time [min]	70	75	75	70
Turnover rate [mmol/h]	5.7	4.0	4.0	4.4

As well as the products of the reaction with the alkali metals, the dried products of the reaction between alkaline earth and rare earth metals with SF_6, were sealed in borosilicate glass tubes for the crystallization at 450 °C over five days in a single zone tube furnace. In the case of Sr, Ba and Eu, the X-ray powder diffraction patterns show the bivalent fluorides $M^{II}F_2$ and sulfides $M^{II}S$. Additionally, byproducts, such as unreacted metal (Ba), amide that converts to nitride during the crystallization process (EuN), or silicon from the glass tube, could be obtained in some reactions. For ytterbium, the trivalent fluoride YbF_3 could be observed next to YbN as a byproduct after crystallization, which suggests the formation of $Yb(NH)_2$ as an intermediate. In all cases, it was not possible to detect elemental sulfur and the addition of diluted HCl lead to the formation of H_2S.

Figure 3 shows the X-ray powder diffraction pattern of the reaction between Sr and SF_6. The lattice parameters of a = 5.8004(6) Å, V = 195.156(3) Å^3 for SrF_2 and of a = 6.0157(7) Å, V = 217.642(3) Å^3 for SrS are in accordance with the results shown in the literature [14,15].

The ATR IR spectrum (Figure S2) shows no bands in the range of 4000 to 400 cm^{-1}. An IR band of SrS should be observed at 185 cm^{-1} and 280 cm^{-1}, so there is no IR activity expected in the measured region [16]. The measured intensities between 2200 and 1900 cm^{-1} are signals from the ATR diamond module (Figure S2).

3. Conclusions

SF_6 reacts readily at −50 °C with dissolved metals (Li–Cs, Sr, Ba, Eu) in liquid ammonia under normal pressure. The reaction leads to mono- or bivalent fluorides and sulfides ($M^{I}F$, M^{I}_2S; $M^{II}F_2$, $M^{II}S$) and, in some cases, byproducts like amides are formed. For Yb, the trivalent fluoride could also be obtained. The method described here represents an elegant and easy path for the decomposition of SF_6, which can be realized for small and, conceivably, for industrial batch sizes. The reactions could offer an opportunity for an effective removal of the existing SF_6-stocks.

4. Materials and Methods

All work was carried out excluding moisture and air in an atmosphere of dried and purified argon (5.0, Praxair, Düsseldorf, Germany) using high-vacuum glass lines and a glovebox (MBraun, Garching, Germany). Liquid ammonia (Gerling Holz & Co., 99.98%, Hamburg, Germany) was dried and stored over sodium (VWR, Germany) in a special high-vacuum glass line with a Hg pressure relief valve. Sulfur hexafluoride (Solvay, 99.9%, Hannover, Germany) was directly passed into the reaction vessel without any further treatment.

The alkali metals Li, Na, K (Merck, >99%, Darmstadt, Germany; Lab Chem Röttinger, >99%, Dinslaken, Germany; Merck 99%) and the alkali earth metals Sr and Ba (Onyxmet, 99%; Onyxmet 99.8%, Olsztyn, Poland) were used as supplied. Rb and Cs were distilled according to Hackspill in a borosilicate glass distillery, which was treated with hot aqua regia several times und flame-dried under vacuum before the distillation [17]. Eu and Yb were extracted several times over a fritt with liquid ammonia in a special Schlenk vessel [18]. All metals were stored in the glove box under argon in closed flasks.

All glass vessels were made of borosilicate glass, and were flame-dried several times under vacuum before use.

For the reactions, the Schlenk vessels were charged with an amount of metal shown in Table 3. About 20–25 mL of the predried liquid ammonia was condensed at −78 °C (Isopropanol/CO_2-bath) onto the metal. An intense blue to metallic bronze color was obtained for the solution. Subsequently, because of the sublimation point of −63.8 °C for SF_6, the mixture was warmed to −50 °C by cooling the vessel with isopropanol and an Ultra-Low Refrigerated-Heating Circulator (Julabo FP 90, Seelbach, Germany). After 50–135 min, the blue colour of the solution disappeared and the liquid ammonia was removed slowly under vacuum.

Table 3. Amounts of alkali, alkaline earth and rare earth metals used for reaction with SF_6 in liquid ammonia.

Metal	m/mg	n/mmol
Li	250	36.0
Na	890	38.7
K	400	10.2
Rb	711	8.3
Cs	647	4.9
Sr	589	6.7
Ba	689	5.0
Eu	753	5.0
Yb	890	5.1

4.1. Powder X-ray Diffraction

The powder X-ray diffraction patterns were recorded at room temperature with a STOE Stadi MP powder diffractometer (STOE, Darmstadt, Germany). The diffractometer used Cu Kα1 radiation, a Ge monochromator and a Mythen1K detector. The samples were powdered in a glovebox under argon atmosphere in agate mortars and sealed into borosilicate capillaries with a diameter of 0.3 mm,

which were flame-dried several times under vacuum before utilization. All samples were charged in the glove box in a flame-dried ampoule (8 mm outer diameter, 1.5 mm wall thickness). A stopcock attached to the ground joint allowed transfer of the ampoule to a Schlenk line. The bottom of the ampoule was cooled with liquid nitrogen, and the ampoules were flame sealed under vacuum (1×10^{-3} mbar). These ampoules were annealed in a tube furnace for 5 days at 450 °C for better crystallization.

The evaluation of the powder X-ray patterns was carried out with the *WinXPOW* software package and the ICDD powder diffraction file database [19,20]. Le Bail fitting and Rietveld refinement were done with JANA 2006 [21].

4.2. IR Spectroscopy

The IR spectra were recorded on a Bruker alpha FT-IR-spectrometer (Bruker Optik GmbH, Rosenheim, Germany) using the ATR Diamond module with a resolution of 4 cm^{-1}. The spectrometer was located inside a glovebox under argon atmosphere. The spectra were processed with the *OPUS* software package [22].

4.3. SEM Imaging

The scanning electron microscopy images were recorded on a JEOL JIB 4610F (Jeol, Freising, Germany), dual beam FIB/SEM with a Schottky thermal files emission gun (acceleration voltage 0.2–30 kV, resolution 1.2 nm at 30 kV, 3.0 nm at 1 kV), a Gallion ion source (acceleration voltage 1–30 kV, resolution 5 nm at kV and a backscattered and secondary electron detector.

Supplementary Materials: The following are available online at www.mdpi.com/2304-6740/5/4/68/s1, Figure S1: IR spectrum of RbF and Rb_2S measured on an ATR diamond module, Figure S2: IR spectrum of SrF_2 and SrS measured on an ATR diamond module.

Acknowledgments: Florian Kraus thanks the Deutsche Forschungsgemeinschaft (DFG) for a Heisenberg professorship. We thank Solvay for the donation of SF_6 and Harms, Marburg, for the X-ray measurement time. For the SEM images we thank Michael Hellwig from the Center of material science of the Philipps-University Marburg.

Author Contributions: Holger Lars Deubner performed the experiments, analyzed the data and wrote the paper. Florian Kraus designed research and analyzed the data.

Conflicts of Interest: The authors declare no conflict of interest.

References

1. Holleman, A.F.; Wiberg, E.; Wiberg, N. *Lehrbuch der Anorganischen Chemie*, 102nd ed.; De Gruyter: Berlin, Germany, 2007; pp. 556–557, ISBN 3110177701.
2. Ko, M.K.W.; Sze, N.D.; Wang, W.C.; Shia, G.; Goldman, A.; Murray, F.J.; Murcray, D.G.; Rinsland, C.G. Atmospheric sulfur hexafluoride: Sources, sinks and greenhouse warming. *J. Geophys. Res. Atmos.* **1993**, *98*, 10499–10507, doi:10.1029/93JD00228.
3. Evans, F.E.; Mani, E. Sulfur fluorides. In *Kirk-Othmer Encyclopedia of Chemical Technology*, 4th ed.; Kroschwitz, J.I., Howe-Grant, B.M., Eds.; John Wiley & Sons: New York, NY, USA, 1994; pp. 428–442.
4. Zámosta, L.; Braun, T.; Braun, B. S–F and S–C Activation of SF_6 and SF_5 Derivatives at Rhodium: Conversion of SF_6 into H_2S. *Angew. Chem. Int. Ed.* **2014**, *53*, 2745–2749, doi:10.1002/anie.201308254.
5. Holze, P.; Horn, B.; Limberg, C.; Matlachowski, C.; Mebs, S. Aktivierung von Schwefelhexafluorid an hoch reduzierten niedrig koordinierten Nickel-Distickstoff-Komplexen. *Angew. Chem. Int. Ed.* **2014**, *53*, 2750–2753, doi:10.1002/anie.201308270.
6. Zang, J.; Zhou, J.Z.; Xu, Z.P.; Li, Y.; Cao, T.; Zhao, J.; Ruan, X.; Liu, Q.; Qian, G. Decomposition of Potent Greenhouse Gas Sulfur Hexafluoride (SF_6) by Kirchsteinite-dominant Stainless Steel Slag. *Environ. Sci. Technol.* **2014**, *48*, 599–606.
7. Moissan, H.; Lebeau, P.C.R. Sur un nouveau corps gazeux: Le perfluorure de soufre SF_6. *Acad. Sci. Paris C. R.* **1900**, *130*, 865–871.

8. Cowen, H.C.; Riding, F.; Warhurst, E.J. The Reaction of Sulphur Hexafluoride with Sodium. *Chem. Soc.* **1953**, 4168–4188, doi:10.1039/JR9530004168.
9. Demitras, G.C.; MacDiarmid, A.G. The Low Temperature Reaction of Sulfur Hexafluoride with Solutions of Sodium. *Inorg. Chem.* **1964**, *3*, 1198–1199, doi:10.1021/ic50018a033.
10. Brewe, L.; Chang, C.; King, B. Sulfur Hexafluoride. Its reaction with Ammoniated Electrons and Its Use as a Matrix for Isolated Gold, Silver and Copper Atoms. *Inorg. Chem.* **1970**, *9*, 814–816, doi:10.1021/ic50086a024.
11. Vouillon, J.C.; Sebaoun, A. Le systéme eau-fluorine de rubidium. *Bull. Soc. Chim. Fr.* **1969**, *36*, 2604–2608.
12. Santamaria Pérez, D.; Vegas, A.; Muehle, C.; Jansen, M. High pressure experimental study on Rb_2S: Antifluorit to Ni_2In-type phase transitions. *Acta Cryst. B* **2011**, *67*, 109–115.
13. Nakamoto, K. *Infrared and Raman Spectra of Inorganic and Coordination Compounds*, 5th ed.; John Wiley & Sons: New York, NY, USA, 1986.
14. Sobdev, D.P.; Kaimov, D.N.; Sul'yanov, S.N.; Zhanorova, Z.J. Nanostructured crystals of fluorite phases $Sr_{1-x}R_xF_{2+x}$ (*R* are rare-earth elements) and their ordering. I. Crystal growth of $Sr_{1-x}R_xF_{2+x}$ (*R* = Y, La, Ce, Pr, Nd, Sm, Gd, Tb, Dy, Ho, Er, Tm, Yb, and Lu). *Crystallogr. Rep.* **2009**, *54*, 122–130.
15. Andreev, O.V.; Kartman, A.V.; Bamborov, V.G. Phase equilibria in the $SrS–Ln_2S_3$ systems (La = La, Nd, Gd). *Russ. J. Inorg. Chem.* **1991**, *36*, 144–146.
16. Kaneko, Y.; Morimoto, K.; Koda, T. Optical Properties of Alkaline-Earth Chalcogenides, I Single Crystal Growth and Infrared Reflection Spectra Due to optical Phonons. *J. Phys. Soc. Jpn.* **1982**, *51*, 2247–2254.
17. Hackspill, L. Sur quelques propriétés des métaux alcalins. *Helv. Chim. Acta* **1928**, *11*, 1003–1026.
18. Nassler, J.; Lagowski, J.J. *The Chemistry of Non-Aqueous Solvents*; Academic Press: New York, NY, USA; London, UK, 1966; Volume 1, p. 214.
19. *STOE WinXPOW*, version 3.07; Stoe & Cie GmbH: Darmstadt, Germany, 2015.
20. *International Centre for Diffraction Data*, *PDF-2 2003 (Database)*; ICDD: Newtown Square, PA, USA, 2003.
21. Petricek, V.; Dusek, M.; Palatinus, L. *Jana 2006–The Crystallographic Computing System*; Institute of Physics: Praha, Czeck Republic, 2017.
22. *OPUS*, version 7.2; Bruker Optik GmbH: Ettlingen, Germany, 2012.